Accurate Numerical Method for Calculating Frequency-Distribution Functions in Solids*

G. GILAT AND L. J. RAUBENHEIMER†
Solid State Division, Oak Ridge National Laboratory, Oak Ridge, Tennessee
(Received 29 November 1965)

A new method of calculating absolute phonon frequency-distribution functions, which is an extension of the extrapolation method developed by Gilat and Dolling, is presented for cubic crystals. The method involves dividing the irreducible section of the first Brillouin zone into a cubic mesh and approximating the constant-frequency surfaces inside every small cube by a set of parallel planes. This method proves to be of high precision and resolution in obtaining fine details associated with a given model, and it requires relatively short computing time. Applications have been made to nickel, aluminum, and sodium, for which there exist satisfactory force-constant models. New critical points have been found for Al at $\nu=7.104\pm0.006$ THz and for Na at $\nu=2.856\pm0.010$ THz. Certain critical points associated with the longitudinal phonon band have been resolved more sharply than in earlier calculations.

I. INTRODUCTION

THE frequency-distribution function $g(\nu)$ of the normal modes of vibration of solid crystals is of key importance for understanding many properties of solids (e.g., thermodynamic properties, infrared scattering, and superconductivity). This distribution function can be obtained directly from experiment[1] for cubic crystals by using incoherent inelastic scattering of slow neutrons. Such experiments have actually been performed on vanadium [2–5] nickel,[5–6] and titanium,[5] which have large cross sections for incoherent scattering. Unfortunately, the energy resolution of these experiments is still too poor to reveal fine details about $g(\nu)$, such as the location of the critical points. Moreover, the number of materials having sufficiently large incoherent cross sections is limited. However, $g(\nu)$ can, in principle, be calculated from the data on coherent inelastic scattering of slow neutrons, which yield the dispersion curves of the normal modes of vibrations.

In order to calculate $g(\nu)$ from the dispersion curves, it is necessary to assume some force model. This is usually obtained by fitting a set of force constants to the dispersion curves and to the elastic constants. These force constants give in return the value of the dynamical matrix at every point $\mathbf{q}$ in the first Brillouin zone of the appropriate reciprocal lattice. Usually the dispersion curves are obtained in high-symmetry directions and then analyzed by the Born–von Kármán theory to obtain the force constants. It might be debated to what extent this theory is able to predict the correct frequencies in off-symmetry directions in view of its possible inadequacy as a good physical description of the dispersion curves. This problem, though serious, is irrelevant to the present article, which is concerned with a new method of computing $g(\nu)$. The method is capable in principle of calculating $g(\nu)$ from any force model, provided the model is able to produce a dynamical matrix at any point $\mathbf{q}$ in the first Brillouin zone. Hence, the validity of the Born–von Kármán theory, which is still the best available theory in many cases, is by no means essential to the method.

Methods for calculating $g(\nu)$ are described at length by Maradudin, Montroll, and Weiss.[7] The simplest and most straightforward is the root-sampling method, in which one solves for the eigenvalues of the dynamical matrix at as many as possible points that form a uniform mesh in the irreducible section of the first Brillouin zone. The main objection to this method is on the grounds of its being slow, since in order to obtain a reasonably good sampling, one needs a very large number of matrix diagonalizations. Gilat and Dolling[8] have recently introduced the so-called "extrapolation method," which increases enormously the sampling size and thus improves considerably the resolution in frequency. This improved resolution allows a better determination of the fine details of the spectrum $g(\nu)$, such as critical points and abrupt changes in slope. The present method is a further extension of the extrapolation method to a point where it effectively extracts "all" frequencies out of the first Brillouin zone. Therefore, it should not be classified as a sampling method, but as a method of calculating absolute $g(\nu)$. This method will be developed here only for cubic systems, but it can be generalized to more complicated systems.

* Research sponsored by the U. S. Atomic Energy Commission under contract with the Union Carbide Corporation.

† Guest scientist from the South African Atomic Energy Board, Pretoria, Republic of South Africa.

[1] G. Placzek and L. Van Hove, Phys. Rev. **93**, 352 (1954).

[2] C. M. Eisenhauer, I. Pelah, D. J. Hughes, and H. Palevsky, Phys. Rev. **109**, 1046 (1958).

[3] A. T. Stewart and B. N. Brockhouse, Rev. Mod. Phys. **30**, 250 (1958).

[4] N. A. Chernoplekov, M. G. Zemlyanov, and A. G. Chicherin, Zh. Eksperim. i Teor. Fiz. **43**, 2080 (1962) [English transl.: Soviet Phys.—JETP **16**, 1472 (1963)].

[5] B. Mozer, K. Otnes, and H. Palevsky, in *Proceedings of the International Conference on Lattice Dynamics, Copenhagen, 1965* edited by R. F. Wallis (Pergamon Press, Inc., New York, 1965), p. 63.

[6] N. A. Chernoplekov, M. G. Zemlyanov, A. G. Chicherin, and B. G. Lyaschenko, Zh. Eksperim. i Teor. Fiz. **44**, 858 (1963) [English transl.: Soviet Phys.—JETP **17**, 584 (1963)].

[7] A. A. Maradudin, E. W. Montroll, and G. H. Weiss, in *Solid State Physics*, edited by F. Seitz and D. Turnbull (Academic Press Inc., New York, 1963), Suppl. 3.

[8] G. Gilat and G. Dolling, Phys. Letters **8**, 304 (1964).

II. THE METHOD

As mentioned in the Introduction, we shall assume that a certain force model is available, from which the elements of a dynamical matrix $D_{ij}^0(\mathbf{q})$ can be derived at every given reduced wave number $\mathbf{q}$ (i, j being indices running from 1 to $3r$, where r is the number of atoms in the primitive unit cell). For simplicity we shall assume that the masses of the different atoms are already included in the expressions of $D_{ij}^0(\mathbf{q})$. In order to obtain the frequencies appropriate to $\mathbf{q}$, one has to solve the following secular equation:

$$|D_{ij}^0(\mathbf{q})-4\pi^2\nu_0^2\delta_{ij}|=0, \tag{1}$$

where δ_{ij} is the Kronecker delta. The dispersion relations at $\mathbf{q}$ will be satisfied by the $3r$ eigenvalues obtained from Eq. (1). Let us denote by $\mathbf{U}(\mathbf{q})$ the unitary matrix (orthogonal for cases with symmetry of inversion) which diagonalizes $\mathbf{D}^0(\mathbf{q})$. The solution for the eigenvalues can be written as

$$\mathbf{U}\dagger(\mathbf{q})\mathbf{D}^0(\mathbf{q})\mathbf{U}(\mathbf{q})=\mathbf{\Lambda}^0(\mathbf{q}), \tag{2}$$

where $\mathbf{\Lambda}^0(\mathbf{q})$ is a diagonal matrix satisfying

$$\Lambda_{jj}^0(\mathbf{q})=4\pi^2\nu_{0j}^2(\mathbf{q}) \quad (j=1, 2, \cdots, 3r). \tag{3}$$

The idea behind the extrapolation method[8] is to solve for the eigenvalues ν_{0j} at evenly spaced points in reciprocal space and then to find other solutions in between by means of a Taylor expansion about each such point for each eigenvalue. By choosing the points for diagonalization sufficiently close together, all of the reciprocal space can be reached by linear extrapolation. In order to obtain such an expansion, it is necessary to calculate the gradient of the frequency $\nu_j(\mathbf{q})$. Among several possible ways to do this, the quickest is a numerical method, in which one applies successively small artificial changes to each of the three Cartesian components of $\mathbf{q}$ and thus derives three slightly modified dynamical matrices $\mathbf{D}^\alpha(\mathbf{q}+\hat{e}_\alpha\delta q_\alpha)$, where $\hat{e}_\alpha$ is a unit vector along the αth Cartesian axis and δq_α a small increment. We then form the changes $\mathbf{\Delta}^\alpha(\mathbf{q})$ in $\mathbf{D}^0$, defined by

$$\Delta_{ij}^\alpha(\mathbf{q})=D_{ij}^\alpha(\mathbf{q}+\hat{e}_\alpha\delta q_\alpha)-D_{ij}^0(\mathbf{q}). \tag{4}$$

By applying perturbation theory one obtains

$$\epsilon_j^\alpha=\Delta_{jj}^{1\alpha}+\sum_{i\neq j}\frac{(\Delta_{ij}^{1\alpha})^2}{\Lambda_{jj}^0-\Lambda_{ii}^0}+\cdots, \tag{5}$$

where ϵ_j^α is the change in the jth eigenvalue of $\mathbf{D}^0(\mathbf{q})$ when the αth component of $\mathbf{q}$ is changed by δq_α. The element $\Delta_{ij}^{1\alpha}$ is given by

$$\Delta_{ij}^{1\alpha}(\mathbf{q})=\{\mathbf{U}\dagger(\mathbf{q})\mathbf{\Delta}^\alpha(\mathbf{q})\mathbf{U}(\mathbf{q})\}_{ij}, \tag{6}$$

to a first-order approximation. As has been shown by Gilat and Dolling,[8] ϵ_j^α can be approximated by $\Delta_{jj}^{1\alpha}$ to a good degree of accuracy, so that Eq. (5) reduces to

$$\epsilon_j^\alpha\cong\Delta_{jj}^{1\alpha}(\mathbf{q}). \tag{7}$$

Using Eqs. (7) and (3), we obtain

$$(\mathrm{grad}_q\nu_j)_\alpha\cong\frac{\delta\nu_j}{\delta q_\alpha}\cong\frac{1}{8\pi^2\nu_{0j}(\mathbf{q})}\frac{\Delta_{jj}^{1\alpha}(\mathbf{q})}{\delta q_\alpha}. \tag{8}$$

In the extrapolation method[8] one determines the value of $\nu_j(\mathbf{q}+\Delta\mathbf{q})$ from the value of $\nu_{0j}(\mathbf{q})$ by using $\mathrm{grad}_q\nu_j$ as obtained from Eq. (8), i.e.,

$$\nu_j(\mathbf{q}+\Delta\mathbf{q})=\nu_{0j}(\mathbf{q})+(\mathrm{grad}_q\nu_j\cdot\Delta\mathbf{q}). \tag{9}$$

In the actual application of the extrapolation method, the irreducible section of the first Brillouin zone is divided into a uniform simple cubic mesh of points $\mathbf{q}_c$ separated by a distance $2b$. Every $\mathbf{q}_c$ is at the center of a small cube throughout which extrapolation is carried out, usually to a finite number of points, by using Eq. (9). This results in a very substantial increase in the total sampling size. Each cube is properly weighted as required by the symmetry of $\mathbf{q}_c$.

With the present method we extract "all" frequencies out of the small cube containing each $\mathbf{q}_c$ and thus obtain a complete frequency distribution from the sum of the contributions of all the cubes. Let us consider one of the eigenfrequencies $\nu_{0j}(\mathbf{q}_c)$ obtained at $\mathbf{q}_c$. In general, this frequency belongs to a constant-frequency surface passing through $\mathbf{q}_c$. By introducing a small change $d\nu$, one can find a new constant-frequency surface to which $\nu_{0j}(\mathbf{q}_c)+d\nu$ belongs. The number of frequencies which lie in the range between $\nu_{0j}(\mathbf{q}_c)$ and $\nu_{0j}(\mathbf{q}_c)+d\nu$ is proportional to the volume of the layer confined by these surfaces. In the present method we assume that linear extrapolation holds good within every small cube; surfaces of constant frequency are then replaced by parallel planes perpendicular to $(\mathrm{grad}_q\nu_j)_{\mathbf{q}=\mathbf{q}_c}$. The volume element dV falling between two such consecutive planes is proportional to the number of frequencies lying between ν_j and $\nu_j+d\nu$, and as $d\nu$ approaches 0, it can be approximated by

$$dV=Sdq, \tag{10}$$

where S is the area of a plane confined by the cube (hereafter to be called cross-section area) and dq is the thickness of the volume element. Our next interest will be to investigate the variation in the cross-section area when a plane with a given normal sweeps across a cube. Let us denote the direction cosines of the gradient in Eq. (8) by l_1, l_2, and l_3; without loss of generality we can assume that[9]

$$l_1\geq l_2\geq l_3\geq 0, \tag{11}$$

since the coordinate system for every small cube can be relabeled accordingly. We also denote by w the distance of any plane from $\mathbf{q}_c$ and the cross-section area

[9] The cases $l_3=0$ and $l_2=l_3=0$ do not pose any difficult analytical problem, and can be worked out easily. However, choosing a shifted mesh (as described in Ref. 8), the case $l_3=0$ can occur only accidentally, i.e., the probability for its exact occurrence is nil, and so it can be ignored.

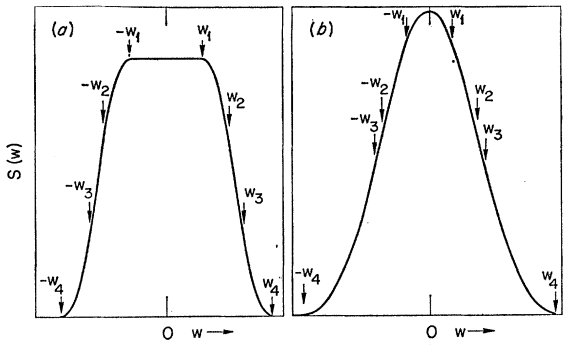

FIG. 1. A typical behavior of the cross section of a cube $S(w)$ as a function of the distance w of the intersecting plane from the cube center. Case (a) represents $l_1>l_2+l_3$ and case (b) is for $l_1<l_2+l_3$.

by $S(w)$. The assumption of linear extrapolation from $\mathbf{q}_c$ implies

$$S(-w)=S(w), \tag{12}$$

so that we have to investigate only one-half of the cube. We choose, quite arbitrarily, the half for which $w>0$. Let us list, in increasing order, the distances of the four corners lying in this half, from the plane passing through the center of the cube:

$$\begin{aligned} w_1&=b|l_1-l_2-l_3|,\\ w_2&=b(l_1-l_2+l_3),\\ w_3&=b(l_1+l_2-l_3),\\ \text{and}\quad w_4&=b(l_1+l_2+l_3), \end{aligned} \tag{13}$$

where $2b$ is the length of the edge of the cube. It is clear that we need to know the behavior of $S(w)$ when w varies in the various ranges defined by (w_{i-1}, w_i), given in Eq. (13). There are two possibilities in the first range $(0,w_1)$, depending on the sign of $(l_1-l_2-l_3)$. If the sign is positive, then the cross section is a parallelogram of area

$$S(w)=4b^2/l_1 \quad \text{for} \quad l_1\geqslant l_2+l_3, \quad (0\leqslant w\leqslant w_1), \tag{14}$$

while if it is negative, the cross section is hexagonal with area

$$S(w)=[l_1l_2l_3]^{-1}[2b^2(l_1l_2+l_2l_3+l_3l_1)-(w^2+b^2)],$$

for

$$l_1<l_2+l_3 \quad \text{and} \quad 0\leqslant w\leqslant w_1. \tag{15}$$

In the next range (w_1,w_2) the shape is a pentagon, the area of which is

$$\begin{aligned} S(w)=[l_1l_2l_3]^{-1}[&2b^2(3l_2l_3+l_1l_2+l_3l_1)\\ &-bw(-l_1+l_2+l_3)-\tfrac{1}{2}(w^2+b^2)]. \end{aligned} \tag{16}$$

For the range (w_2,w_3) we have a quadrangle of area

$$S(w)=2[l_1l_2l_3]^{-1}[b^2l_3(l_1+l_2)-bwl_3]; \tag{17}$$

and finally for (w_3,w_4) we obtain a triangle giving

$$S(w)=[2l_1l_2l_3]^{-1}[b(l_1+l_2+l_3)-w]^2. \tag{18}$$

These expressions, as well as their first derivatives, are all continuous at their respective boundaries and the integral of $S(w)$ over the total range yields the volume of the cube. Equation (12) implies that $S(w)$ is an even function of w, so that for $w<0$, w should be replaced by its absolute value. In Fig. 1 we show schematically a typical behavior of $S(w)$ as w varies over the different ranges. The figure on the left-hand side refers to the case satisfying Eq. (14), whereas the second figure illustrates the case given by Eq. (15). The variation of a frequency ν obtained from $\nu_{0j}(\mathbf{q}_c)$ by extrapolating throughout the cube is given by

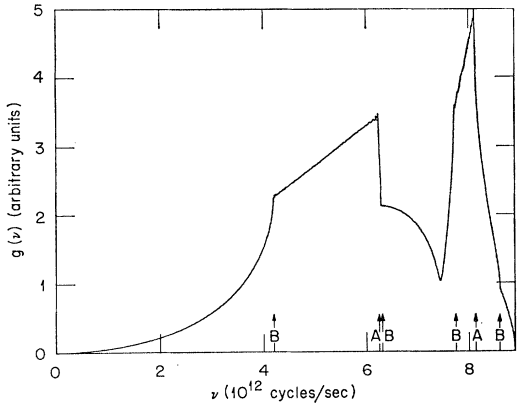

FIG. 2. Unsmoothed computer plot of the frequency-distribution function for Ni at 300°K, obtained from a model by Birgeneau *et al.* (Ref. 10). Frequency range is divided into about 4500 intervals of width 0.002 THz. The various critical points are marked by arrows and indices A and B are explained in the text.

$$\nu=\nu_{0j}(\mathbf{q}_c)\pm w|\operatorname{grad}_q\nu_j|_{q=q_c}, \tag{19}$$

where $0\leqslant w\leqslant w_4$.

In order to construct $g(\nu)$ let us define a function $g(j,\mathbf{q}_c;\nu)$, which is the distribution of frequencies obtained from $\nu_{0j}(\mathbf{q}_c)$ by extrapolating throughout the cube centered at $\mathbf{q}_c$. Assuming that the density of frequencies in reciprocal space is a constant, we obtain

$$\begin{aligned} g(j,\mathbf{q}_c;\nu)d\nu=CW_{q_c}S(w)dw \text{ for } &\nu_{0j}-w_4|\operatorname{grad}\nu_j|_{q_c}\\ &\leqslant\nu\leqslant\nu_{0j}+w_4|\operatorname{grad}\nu_j|_{q_c},\\ =0 \qquad &\text{elsewhere} \end{aligned} \tag{20}$$

where ν and w are linked by Eq. (19). W_{q_c} is a weight factor associated with the symmetry of $\mathbf{q}_c$, and C is an arbitrary number which is constant throughout the entire Brillouin zone. The complete $g(\nu)$ is now given by

$$g(\nu)=\sum_{j,q_c} g(j,\mathbf{q}_c;\nu), \tag{21}$$

where the summation is extended over all eigenvalues and cubes. In practice the entire range of frequencies is divided into very small but finite intervals $(\nu, \nu+d\nu)$ so that the calculated $g(\nu)$ is a histogram which consists of a very large number of channels. While it has been

customary in sampling methods to indicate the sampling size by some number, which is usually proportional to the number of frequencies included in the sample of $g(\nu)$, it becomes meaningless in the present method to do so. In this method the entire Brillouin zone and not just a finite number of selected points contributes to $g(\nu)$.

III. APPLICATIONS

The method described above has been applied to calculate $g(\nu)$ for three elements (namely Ni, Al, and Na), for which there exist Born–von Kármán force models. These force models give very good agreement with data obtained from inelastic coherent scattering of slow neutrons. The curves of $g(\nu)$ in Figs. 2, 3, and 4 are the actual computer plots without any smoothing. The intervals $(\nu, \nu+d\nu)$ for which $g(\nu)$ has been calculated are much smaller than typical intervals used in earlier calculations and are, in fact, limited mainly by the memory capacity of the computer. Nevertheless, $g(\nu)$ is smoothly varying from channel to channel. Such small intervals allow in principle a much better resolution of peaks and critical points in the spectrum, but obviously

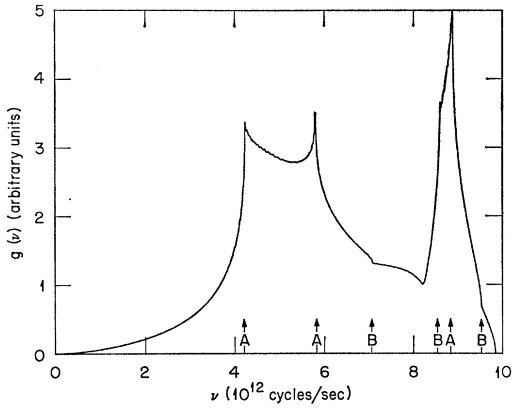

FIG. 3. Unsmoothed computer plot of the frequency-distribution function for Al at 80°K, obtained from a model by Gilat and Nicklow (Ref. 12) based on dispersion curves measured by Stedman and Nilsson (Ref. 13). Frequency range is divided into about 5000 channels of width 0.002 THz. Critical points are marked by arrows and classified as explained in the text.

there are several sources of error connected with various approximations, which might give rise to spurious spikes and fluctuations. In many cases these erroneous details can be eliminated by repeating the calculation with a slightly different mesh. In Sec. IV we discuss these points in more detail.

In all calculations to be described, the dynamical matrix has been diagonalized at points $\mathbf{q}_c$, which form a uniform shifted mesh over the 1/48 irreducible section of the first Brillouin zone. The shifted mesh is useful for avoiding many degeneracies in the dynamical matrix,[8] which are required by symmetry. If n is the number of intervals into which we divide the longest axis (say q_x, where $0 \leqslant q_x \leqslant 1$) of the irreducible section, then b, which is half the side length of every small cube, is

$$b = 1/2n. \tag{22}$$

The αth Cartesian component of the center $\mathbf{q}_c$ of such a cube on a "shifted" mesh is

$$q_\alpha = (m_\alpha - \tfrac{1}{2})2b, \tag{23}$$

where the m_α are all nonzero integers, and $1 \leqslant m_x \leqslant n$. The boundary conditions for m_y and m_z are chosen to match the requirements of the symmetry involved (e.g., bcc or fcc). In practice we have used a finer mesh at small $\mathbf{q}_c$ to improve the reliability of $g(\nu)$ for low frequencies, so that the number of diagonalizations was actually somewhat larger. By using this method, $g(\nu)$ has been calculated for Ni and Al, which are face-centered cubic, and for Na, which is body-centered cubic. The number of matrix diagonalizations required to obtain the fine details displayed by Figs. 2, 3, and 4 was slightly higher than 3000 and for each element about 20 min. computing time was required on the Oak Ridge National Laboratory CDC 1604-A computer. It is, however, possible to obtain a quite satisfactory $g(\nu)$ (e.g., for the purpose of calculating specific heat) using only about 600 diagonalizations. In the following calculations we state the results to quite a high apparent precision. This precision has little meaning because the experimental uncertainty is considerably larger. Nevertheless, in order to display the extent to which it is possible to produce fine features associated with a given model, we have chosen to quote these calculated numbers to such precision. The details of each calculation are described in the following paragraphs.

A. Nickel

The calculation of $g(\nu)$ is based on a general four-nearest-neighbor force model obtained from a best fit

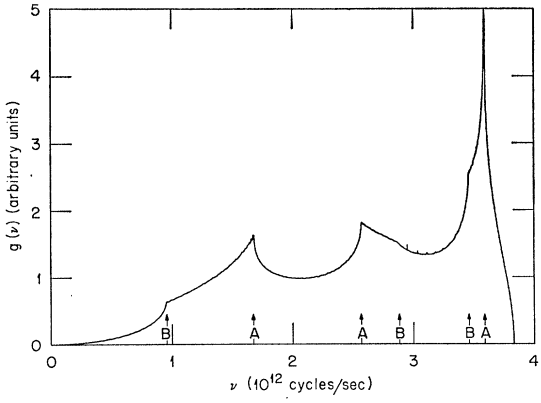

FIG. 4. Unsmoothed computer plot of the frequency-distribution function for Na at 90°K, obtained from a model by Woods *et al.* (Ref. 14). Frequency range is divided into about 4000 intervals of width of 0.001 THz. Critical points are identified as explained in the text.

to the phonon dispersion curves at 300°K by Birgeneau *et al.*[10] The plot of $g(\nu)$ is shown in Fig. 2. It was obtained from 3199 matrix diagonalizations using $n=32$. The frequency interval was $d\nu=0.002$ THz (1 THz$=10^{12}$ cps), so that $g(\nu)$ was sorted into about 4500 intervals. The small wriggles on the graph are probably due to computational errors, which are discussed in Sec. IV. We classify[11] the different kinds of critical points in $g(\nu)$ into two categories: (A) critical points which show up as spikes, and (B) critical points at which there is only an abrupt change of slope. The critical points in Fig. 2 are at the following frequencies in units of THz: 4.215±0.004 (B), 6.243±0.004 (A), 6.296±0.004 (B), 7.742±0.004 (B), 8.118±0.004 (A), and 8.616±0.008 (B).

B. Aluminum

The computation of $g(\nu)$ is based on an axially symmetric Born–von Kármán eight-nearest-neighbor model derived by Gilat and Nicklow,[12] who analyzed the phonon-dispersion curves obtained by Stedman and Nilsson[13] at 80°K. The technical details concerning the computation of $g(\nu)$ are identical with those of Ni. The number of intervals in this case was approximately 5000. The plot of $g(\nu)$ is shown in Fig. 3 and the critical points are at the following frequencies in units of THz: 4.236±0.006 (A), 5.802±0.003 (A), 7.104±0.006 (B), 8.622±0.004 (B), 8.879±0.003 (A), and 9.534±0.006 (B). The point at 7.104, although weak, has been clearly resolved.

C. Sodium

The force model for the phonon dispersion curves was taken from Woods *et al.*[14] It is a general five-nearest-neighbor model obtained from data taken at 90°K. Sodium, being a bcc crystal, has a first Brillouin zone with a different shape from that of Ni and Al. The number of diagonalizations was 3287, and the mesh number was $n=40$. The frequency interval was $\Delta\nu=0.001$ THz, which yielded almost 4000 frequency channels. The frequency-distribution function $g(\nu)$ is shown in Fig. 4, and critical points are at the following frequencies: 0.949±0.003 (B), 1.672±0.002 (A), 2.573±0.003 (A), 2.856±0.010 (B), 3.462±0.003 (B), and 3.591±0.002 (A). The critical point at 2.86 has apparently not been observed before. The one at 3.46 is resolved more clearly than by Dixon *et al.*,[15] who used the ordinary sampling method. The shape of the main peak is also somewhat different from that calculated by Dixon *et al.*

It might be of some interest to point out that in all three cases discussed above (and presumably for most of the fcc and bcc monatomic crystals) there exists a clearly resolved critical point of type B at a frequency slightly smaller than that of the highest peak. This frequency is probably associated with the maximum observed for some of the dispersion curves along the high-symmetry directions. It usually occurs along $L(qqq)$ for bcc crystals and along $L(qq0)$ for fcc crystals. These critical points were just barely resolved in earlier calculations.[10,12,15]

IV. DISCUSSION

It would perhaps be of interest at this stage to list the different sources of error involved in the application of the present method, although it is very difficult to make any quantitative estimate of these errors. By summing over so many contributions from all of the cubes and all of the eigenfrequencies, any single error is averaged out to a large extent, so that all errors to be mentioned are perhaps of much less significance than it might appear.

The most important error is probably associated with the use of linear extrapolation. Employing nonlinear higher order terms does not necessarily correct the error, because an approximation is already involved in calculating the first-order term itself. This error is probably the main reason for the small kinks that might be observed on the various plots of $g(\nu)$, and it can largely be eliminated by computing $g(\nu)$ for two slightly different values of n and comparing the kinks for the two meshes.

A second kind of error is associated with possible degeneracies in the eigenfrequencies. There are two different types of degeneracies: (a) those required by symmetry and (b) those occurring accidentally. The second type can be dismissed, since the probability for its exact occurrence is zero, and one can avoid its approximate occurrence (quasidegeneracy) by choosing a sufficiently small δq_α in Eq. (8). The degeneracies required by symmetry are more important. It has been shown[8] that when a shifted mesh of $\mathbf{q}_c$ is chosen so that none of the components of $\mathbf{q}_c$ is equal to zero, most of the high-symmetry branches are automatically excluded. We are left only with the branch $q_{cx}=q_{cy}=q_{cz}$ of relatively low weight, which has two degenerate transverse modes. One can partially overcome this problem by using numerical devices, but in any event, the averaging process makes this error unimportant, except for the acoustic contributions of the cube at the origin. This cube is the only contributor to $g(\nu)$ at $\nu\to 0$. Fortunately, this is exactly the region where the Debye approximation for

[10] R. J. Birgeneau, J. Cordes, G. Dolling, and A. D. B. Woods, Phys. Rev. **136**, A1359 (1964).

[11] We use this classification for purely practical reasons. One has to analyze the computed data somewhat differently to obtain points of types (A) and (B), respectively. This is by no means intended to replace the widely used classification of critical points based on topological analysis (for instance, see Ref. 7).

[12] G. Gilat and R. M. Nicklow, Phys. Rev. **143**, 487 (1966).

[13] R. Stedman and G. Nilsson, in *Inelastic Scattering of Neutrons in Solids and Liquids* (International Atomic Energy Agency, Vienna, 1965), Vol. I, p. 211.

[14] A. D. B. Woods, B. N. Brockhouse, R. H. March, and A. T. Stewart, Phys. Rev. **128**, 1112 (1962).

[15] A. E. Dixon, A. D. B. Woods, and B. N. Brockhouse, Proc. Phys. Soc. (London) **81**, 973 (1963). See also the calculation reported in Ref. 8.

$g(\nu)$ is valid, and one can simply extrapolate $g(\nu)$ at $\nu \rightarrow 0$ from slightly higher ν, assuming that $g(\nu)$ is proportional to ν^2.

A third source of error, probably less significant, is associated with neglecting higher order contributions to the gradient by the use of Eq. (7) instead of Eq. (5). This error becomes more pronounced when one is close to some degeneracy, but if such a quasidegeneracy actually occurs, not even Eq. (5) is necessarily valid, since it may not converge. However, this error is probably not serious, because such degeneracies are generally not associated with very small gradients, so that the process of averaging out is more effective.

A fourth source of error originates from the finite width of the frequency intervals $d\nu$ when $g(\nu)$ is sorted into channels $(\nu, \nu+d\nu)$. The reason for this error is that the shapes in Fig. 1 are approximated by a set of rectangles of constant width. Since the length of the base of these shapes, when translated to ν, is proportional to $|\mathrm{grad}\nu|$ (see Eq. 19), the error will increase as the gradient becomes smaller. This error, however, has been overcome by computational devices such as the use of an auxiliary smaller interval $d\nu'$, and hence it does not contribute appreciably.[16]

It is clear that the magnitude of $1/|\mathrm{grad}\nu|$ is a decisive factor in causing computational errors. However, the occurrence of $|\mathrm{grad}_q \nu_j|_{q=q_c}=0$ is not too serious, since it does not cause an infinity in $g(\nu)$ because of the finite interval $d\nu$. It would be better, though, to avoid zero gradients as far as possible, because they magnify errors that may originate from other causes. Again, as is the case for degeneracies, zero gradients can occur either by symmetry or accidentally. The use of a shifted mesh avoids the former completely, while the probability of the occurrence of the latter is zero.

[16] The only case among the three presented here where corrective steps were really necessary was Na, for which the absolute value of the frequency gradient is particularly small over a large portion of the Brillouin zone. This is also the reason for the sharpness of the major (longitudinal) critical point displayed by Na in comparison to Ni and Al.

The main advantage of this method seems to be its remarkable resolution in energy. As demonstrated by the applications for Na, Al, and Ni, the resolution is at least a factor of 20 better than that obtained by any other method. A secondary advantage is the requirement of less computing time than with the former extrapolation method, since for the same n, there is a gain in time of 30% or more. Another advantage, which holds for both extrapolation methods as compared with the root-sampling method, is that they become more and more efficient the larger the number of atoms per unit cell. This gain in efficiency occurs, because by extrapolation one obtains much more data per diagonalization, which allows substantial reduction in the number of diagonalizations needed to attain the same statistical accuracy. For this reason we also believe that this method might be of considerable help in calculating electronic density of states from results of band structure calculations.

In conclusion, we would like to raise a question concerning the physical nature of phonon frequency-distribution functions. In calculating $g(\nu)$, one usually employs the harmonic approximation, which gives infinitely sharp normal modes of vibration. More realistic models, however, must include anharmonic contributions, which give rise to phonon linewidths. These widths are generally functions of both $\mathbf{q}$ and ν, and thus will affect $g(\nu)$ in a very complicated manner. Strong anharmonic effects will presumably blur fine details in the spectrum, and this problem has yet to be treated quantitatively.

ACKNOWLEDGMENTS

We wish to thank Dr. R. M. Nicklow and Dr. M. K. Wilkinson for many helpful discussions. One of us (L.J.R.) wishes to thank the Oak Ridge National Laboratory for its hospitality. The FORTRAN program used for these calculations is described in Oak Ridge National Labaratory Report No. TM-1425 (unpublished)